JACS
JOURNAL OF THE AMERICAN CHEMICAL SOCIETY
Communication
pubs.acs.org/JACS

A Janus Chelator Enables Biochemically Responsive MRI Contrast with Exceptional Dynamic Range

Eric M. Gale,* Chloe M. Jones, Ian Ramsay, Christian T. Farrar, and Peter Caravan

The Athinoula A. Martinos Center for Biomedical Imaging, The Institute for Innovation in Imaging, Department of Radiology, Massachusetts General Hospital, Harvard Medical School, 149 Thirteenth Street, Suite 2301, Charlestown, Massachusetts 02129, United States

Supporting Information

ABSTRACT: We introduce a new biochemically responsive Mn-based MRI contrast agent that provides a 9-fold change in relaxivity via switching between the Mn^{3+} and Mn^{2+} oxidation states. Interchange between oxidation states is promoted by a "Janus" ligand that isomerizes between binding modes that favor Mn^{3+} or Mn^{2+}. It is the only ligand that supports stable complexes of Mn^{3+} and Mn^{2+} in biological milieu. Rapid interconversion between oxidation states is mediated by peroxidase activity (oxidation) and L-cysteine (reduction). This Janus system provides a new paradigm for the design of biochemically responsive MRI contrast agents.

Molecular magnetic resonance imaging (MRI) adds a dimension of biochemical specificity to the rich anatomic and physiological data attainable through MRI.[1,2] Biochemical specificity is achieved either by conjugating an MRI contrast agent to a targeting vector or engineering the contrast agent to undergo a change in magnetic relaxation (or "activation") in the presence of a biochemical stimulus. Innovative chemistry has generated molecular MRI contrast agents capable of detecting protein targets,[3] pH changes,[4] redox activity,[5] hypoxia,[6] ion fluxes,[7] neurotransmitters,[8] necrosis,[9] and enzyme activity.[10]

Sensitivity, dynamic range, and rate of response are the three main challenges to developing molecular MRI contrast agents. T_1 relaxation agents are detected at ≥10 μM (metal ion), and thus, only a handful of cellular and protein targets are candidates for imaging with targeted agents.[1] Activatable agents suffer from poor dynamic range. With a few notable exceptions,[3,11,12] activatable Gd-based agents rarely achieve >2-fold r_1 change in the presence of physiologically relevant levels of biochemical stimuli. Often, activatable contrast agents require prolonged incubation times before measurable relaxation change is observed. Elegant examples of activatable agents detected via changes in the chemical exchange saturation transfer (CEST) effect have been reported,[4] but these agents are typically detected with far lower sensitivity than T_1 agents.[1]

Although comparatively underexplored, coordination complexes that undergo a biochemically mediated change in paramagnetism offer a promising strategy to expand the dynamic range of activatable probes.[13−15] We and others have pursued biochemically activated MRI contrast agents that utilize the $Mn^{3+/2+}$ couple as the activation mechanism.[16−20] The $Mn^{3+/2+}$ couple is physiologically tenable and can be tuned through ligand modifications.[21] High-spin Mn^{2+} is a potent relaxation agent, whereas Mn^{3+} is a much less effective relaxation agent.[22]

Rational design of redox-activated Mn-based contrast agents is challenging. Most ligand systems support a single oxidation state. Poly(aminocarboxylate) chelators like BPED (Chart 1) and EDTA bind Mn^{2+} with high affinity (Table S1),[23] but the redox potentials of the corresponding Mn^{3+} complexes are very high, causing them to decompose within seconds in aqueous media.[24] Mn^{3+} is stabilized by strongly electron-releasing ligands like HBED (Chart 1) and TPPS (Figure S1). Coordination of Mn^{2+} by these ligands triggers spontaneous oxidation to Mn^{3+}.[18,25] The HBET ligand (Figure S1) stabilizes both oxidation states, but the $Mn^{3+/2+}$ redox potential is >0.50 V more positive than that of tissues and cells.[26,27] Although Mn^{3+}−HBET can be prepared and is stable in aqueous solution, it does not persist in blood plasma (Figures S2 and S3).

Chart 1. (A) The Mn^{3+}- and Mn^{2+}-Selective Chelators HBED and BPED, Respectively, and the Janus Chelate (JED) Designed To Support Both Mn^{3+} and Mn^{2+}; (B) Redox-Triggered Isomerization of Mn^{3+}− and Mn^{2+}−JED

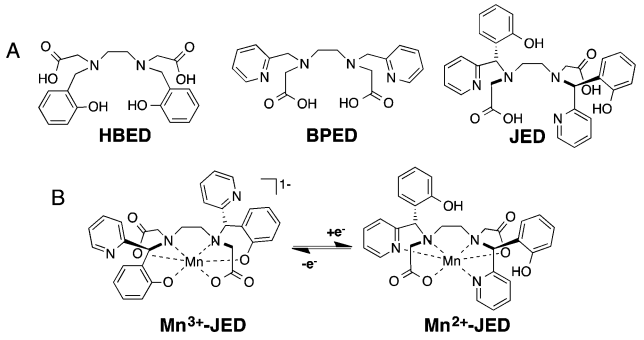

We hypothesized that we could stabilize both oxidation states using a ligand that isomerizes between Mn^{3+}- or Mn^{2+}-selective chelators. Our prototype ligand to test this strategy, JED (short for "Janus HBED/BPED") (Chart 1), is designed to present an HBED-type donor set to Mn^{3+} and a BPED-type donor set to Mn^{2+}. Upon oxidation or reduction, the opposite Janus face will

Received: October 21, 2016
Published: November 24, 2016

DOI: 10.1021/jacs.6b10898
J. Am. Chem. Soc. 2016, 138, 15861−15864

capture the otherwise unstable oxidation state. By analogy with previously characterized Mn^{2+} complexes with acyclic hexadentate chelators, we anticipated that the Mn^{2+} complex would form a seven-coordinate ternary complex with a rapidly exchanging water coligand, a requisite for high relaxivity.[28,29] The smaller Mn^{3+} ion is expected to be six-coordinate with no inner-sphere water ligand and low relaxivity, analogous to the related $[Mn(EHPG)]^-$complex (Figure S1).[30]

Diasteromerically pure JED (*R,R/S,S*) was isolated following a seven-step synthesis (Scheme 1). Aldol reaction of phenol and 2-pyridinecarboxaldyde to give **1** followed by SeO_2 oxidation yielded the synthon for the Janus pyridyl-N/phenolato-O donor **2**. Double condensation of **2** with ethylenediamine yielded **3**, which was reduced with $NaBH_4$ to obtain a diastereomeric mixture of diamine **4**. Preparative separation of the diastereomers of **4** proved difficult, but facile separation was achieved after Zn chelation (Figures S4 and S5). Zn was stripped from the diastereomerically pure **4** with excess DTPA at pH 5.0. Introduction of the acetate-O donors via reductive amination of (*R,R/S,S*)-**4** with glyoxylic acid yielded JED. The Mn^{2+} and Mn^{3+} complexes were independently synthesized via reactions of JED with $MnCl_2$ and MnF_3, respectively.

Scheme 1. Synthesis of JED[a,b]

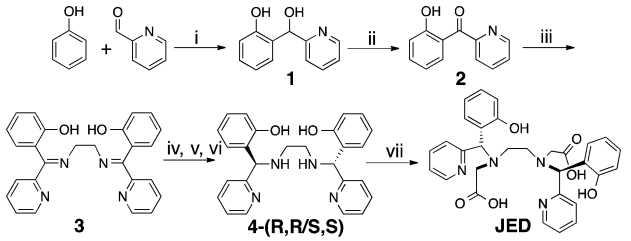

[a]Conditions: (i) $MgCl_2$, Me_2NEt, CH_2Cl_2, RT; (ii) SeO_2, dioxane, 100 °C; (iii) 0.5 molar equiv of ethylenediamine, MeOH, RT; (iv) $NaBH_4$, MeOH; (v) $Zn(OTf)_2$, 1:1 MeCN/H_2O, RT, diastereomers of Zn·**4** were separated by RP-HPLC; (vi) excess DTPA, pH 5.0; (vii) glyoxylic acid, $NaBH_3CN$, $NaHCO_3$, MeOH. [b]JED was prepared from the (*R,R/S,S*) diastereomer of **4**; (*S,S*)-**4** and JED are depicted here.

"BPED-type" binding of Mn^{2+} was confirmed by UV−vis spectroscopy. Prior work with HBET and Mn^{2+}−HBET complexes showed that phenol ionization is accompanied by a significant red shift that can be used to track phenolato-O coordination.[17] JED exhibits a similar red shift (268 to 308 nm) at pH > 10 (Figure S9). The absorbance profile of Mn^{2+}−JED shows no evidence of phenol ionization out to pH 8 (Figure S10). The Mn^{3+} complex can exist only if the Janus switch to "HBED-type" binding occurs. HBED-type binding to Mn^{3+} was further evidenced by UV−vis spectroscopy. The Mn^{3+}−JED ligand-to-metal charge transfer (LMCT) transitions (Figure S12) reflect those of known Mn^{3+} complexes of ligands similar to HBED.[30]

Cyclic voltammetry measurements performed on Mn−JED reveal irreversible oxidation and reduction events (Figure S11). From these data we estimate that the oxidation and reduction potentials are 0.91 and 0.01 V vs NHE, respectively. The Mn−JED oxidation and reduction events mirror the Mn^{2+}−BPED oxidation event (1.11 V) and the Mn^{3+}-HBED reduction event (−0.17 V) (Table S1).

The thermodynamic stability of Mn^{2+}−JED was evaluated by monitoring the direct competition reaction with BPED (log $K_{pH\ 7.4}$ = 11.2; Table S1) using HPLC (0.1 M KNO_3, RT), which yielded log $K_{pH\ 7.4}$ = 10.8 ± 0.2 for Mn^{2+}−JED. Mn^{2+}−JED is among the most stable Mn^{2+} complexes reported (Table S1). Direct measurement of Mn^{3+} formation constants is challenging because the Mn^{3+} aqua ion spontaneously disproportionates to Mn^{2+} and Mn^{4+} in water. Instead, the Mn^{3+}−JED formation constant, log $K_{pH\ 7.4}$ = 28.6, was estimated from the Mn^{2+}-JED formation constant and the redox potentials[31] (eq S3). For comparison, the value log $K_{pH\ 7.4}$ = 29.4 is estimated for Mn^{3+}−HBED. The congruence of the Mn^{2+}− and Mn^{3+}−JED formation constants with those of Mn^{2+}−BPED and Mn^{3+}−HBED, respectively, provides additional evidence of BPED- and HBED-type JED coordination.

The Mn^{2+} complex is a much stronger relaxation agent than its Mn^{3+} sister complex. Relaxivity values were recorded in water and human blood plasma at 1.4, 4.7, and 11.7 T at 37 °C (Table 1). The $r_1^{Mn^{2+}}/r_1^{Mn^{3+}}$ ratios are among the largest measured for any reported activatable Gd- or Mn-based relaxation agent, with a 9-fold change measured in human plasma at 1.4 T. For Gd-based agents, the largest dynamic ranges reported are achieved via reactions to form products that constrain the Gd rotational dynamics.[11,12] Altering the rotational dynamics provides a profound effect at field strengths ≤1.5 T but is nearly obsolete by 3.0 T.[32] Mn−JED maintains a 3.3−5.0-fold r_1 change at 4.7 and 11.7 T. The higher relaxivity of the Mn^{2+} complex is consistent with a tertiary complex with a rapidly exchanging water coligand, while the lower relaxivity of the Mn^{3+} complex is consistent with a coordinately saturated complex that precludes water coordination. The increase in relaxivity observed in blood plasma at 1.4 T suggests some degree of protein binding.

Table 1. Relaxivity Values (r_1) of Mn^{3+}− and Mn^{2+}−JED Recorded in Water or (in Parentheses) Human Plasma at 1.41, 4.7,[a] and 11.7 T at 37 °C; The Relaxivity of Mn^{2+}−JED Is Much Higher Regardless of Applied Field Strength

	Mn^{3+}	Mn^{2+}	$r_1^{Mn^{2+}}/r_1^{Mn^{3+}}$
1.4 T	0.5 ± 0.01 (0.9 ± 0.01)	3.3 ± 0.06 (8.0 ± 0.39)	6.6 (8.9)
4.7 T[a]	0.9 ± 0.02 (1.1 ± 0.05)	4.3 ± 0.32 (3.6 ± 0.21)	4.8 (3.3)
11.7 T	0.5 ± 0.01 (0.5 ± 0.02)	2.5 ± 0.08 (1.9 ± 0.08)	5.0 (4.8)

[a]Measurements at 4.7 T were performed at RT.

Independently isolated Mn^{3+}− and Mn^{2+}−JED persist in human blood plasma at 37 °C with little interconversion over the course of 24 h. Mn speciation was evaluated by HPLC interfaced to an inductively coupled plasma (ICP) mass spectrometer for Mn detection (Figure 1). Some interconversion between oxidation states was observed, but the reaction

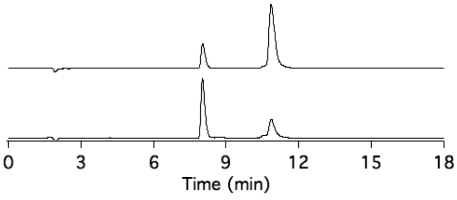

Figure 1. HPLC−ICP-MS traces showing Mn speciation of solutions of (top) Mn^{2+}−JED and (bottom) Mn^{3+}−JED incubated for 24 h at 37 °C in human blood plasma. Mn^{3+}− and Mn^{2+}−JED elute at 8.0 and 10.9 min, respectively. Interconversion between the Mn^{3+} and Mn^{2+} complexes is slow and does not reach equilibrium within 24 h.

DOI: 10.1021/jacs.6b10898
J. Am. Chem. Soc. 2016, 138, 15861−15864

proceeds slowly. Comparison of the resultant 24 h HPLC traces indicates that equilibrium had not yet been achieved. Both complexes are very stable in plasma; >95% of the Mn is present as JED complexes at 24 h.

Peroxidase enzymes amplify the reactivity of reactive oxygen species. High peroxidase activity is a salient feature of the acute inflammatory response, and molecular imaging of peroxidase has been pursued in animal models of vasculitis, stroke, aneurism, and myocardial infarction.[33−36] Peroxidase activities of up to 250 units/mg (~250 000 units/mL) have been measured in atherosclerotic lesions,[37] while here we show that Mn^{2+}−JED to Mn^{3+}−JED conversion is rapidly mediated by peroxidase activity 4 orders of magnitude lower than what is observed in vivo. HPLC traces recorded before and after H_2O_2/peroxidase incubation confirm that conversion to Mn^{3+}−JED occurs without byproducts (Figure 2A). Peroxidase-mediated

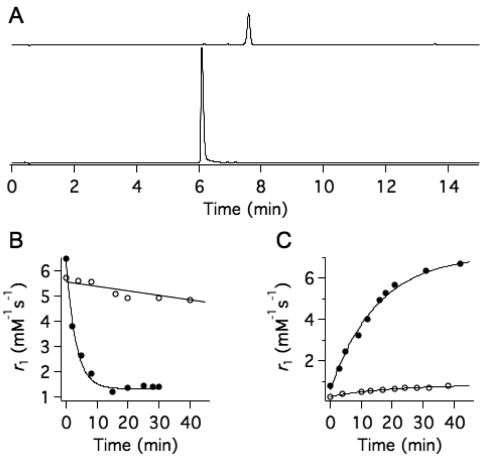

Figure 2. Biochemically mediated interconversion of Mn−JED oxidation states by peroxidase and thiols. (A) Conversion of Mn^{2+}−JED (top trace, 7.6 min) to Mn^{3+}−JED (bottom trace, 6.1 min) triggered by H_2O_2/peroxidase (25 units/mL) in phosphate-buffered saline monitored by HPLC with 254 nm detection. The difference in peak heights for the pre- and post-peroxidase-treated samples results from the 2-fold higher extinction coefficient of Mn^{3+}−JED. (B) Oxidation of Mn^{2+}−JED in the presence of H_2O_2 (○) or H_2O_2/peroxidase (15 units/mL, ●) in human blood plasma as monitored by NMR spectroscopy. H_2O_2 was generated in situ by the glucose/glucose oxidase reaction. (C) Reduction of Mn^{3+}−JED in human blood plasma without (○) and with 5 molar equiv of L-Cys added (●). Relaxometry measurements were performed at 1.4 T and 37 °C.

oxidation of Mn^{2+}−JED is rapid (k_{obs} = 19.1 ± 4.75 s^{-1}) in human blood plasma supplied with a steady state of H_2O_2 via the glucose/glucose oxidase reaction (Figure 2B). Peroxidase-mediated oxidation to Mn^{3+}−JED occurs on the order of seconds, whereas in blood plasma the interconversion between oxidation states occurs on the order of days. H_2O_2 alone triggers negligible conversion, further underscoring the selectivity for peroxidase-mediated oxidation. The rate measured using r_1 changes tracks with the rate measured by optical absorbance at 450 nm (ε = 1180 M^{-1} cm^{-1} for Mn^{3+}−JED) (Figures S12 and S13).

Proliferating tumors are characterized by regions of hypoxia[38] and thiol-rich microenvironments.[39,40] Mn^{3+}−JED is readily reduced to Mn^{2+}−JED in the presence of thiols. Figure 2C depicts the cysteine-mediated reduction of Mn^{3+}−JED by incubation with 5 molar equiv of L-Cys in blood plasma with k_{obs} = 3.60 ± 0.50 s^{-1}. L-Cys reduction results in a remarkable 8.5-fold increase in r_1.

The MRI contrast between equimolar solutions of Mn^{2+}−JED and Mn^{3+}−JED is profound. Figure 3A shows a

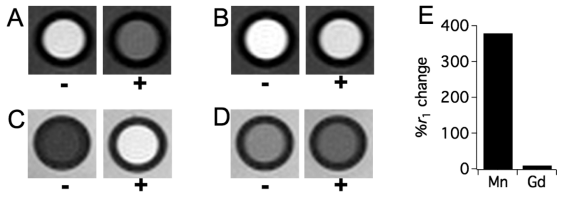

Figure 3. MR phantom images at 4.7 T and RT of water containing 0.5 mM (A, C) Mn^{2+}−JED or (B, D) Gd-bis-5HT-DTPA before (−) and after (+) incubation with H_2O_2/peroxidase (45 units/mL). Images acquired (A, C) using a T_1-weighted FLASH sequence or (B, D) with a 325 ms inversion prepulse to generate large positive contrast in the oxidized sample; see the Supporting Information (SI) for image acquisition details. The high contrast between the samples containing Mn^{2+}−JED and Mn^{3+}−JED and the low contrast for the Gd-based system should be noted. (E) Percentage r_1 changes after peroxidase-mediated oxidation of the Mn- and Gd-based agents. A detailed description of the scanning parameters is given in the SI.

conventional T_1-weighted image at 4.7 T of phantoms containing 0.5 mM Mn^{2+}−JED before (−) and after (+) peroxidase-mediated oxidation. In this image, the higher-relaxivity Mn^{2+}−JED solution is much brighter than the lower-relaxivity Mn^{3+}−JED solution. Gd-bis-5HT-DTPA is a state-of-the-art peroxidase-sensing Gd-based agent whose relaxivity change is mediated by a change in rotational correlation time upon oxidation (Figure S14).[41] However, at 4.7 T oxidation results in only a 15% r_1 change, and this small difference is highlighted in the image in Figure 3B. By using an inversion prepulse we can generate positive contrast in the oxidized Mn^{3+}−JED complex. Figure 3C shows the same phantoms as in Figure 3A imaged with a 325 ms inversion prepulse. The inversion time was chosen to null the signal in the untreated sample, generating large positive contrast in the oxidized sample. Figure 3D shows the same inversion prepulse sequence applied to the Gd-bis-5HT-DTPA samples from Figure 3B. Regardless of the scanning protocol, the contrast generated following oxidation of the Mn-based agent is much larger than that possible with the Gd-based agent. Figure 3E compares percentage r_1 changes observed after peroxidase oxidation of Mn−JED and Gd-bis-5HT-DTPA at 4.7 T. The Mn agent undergoes an r_1 change of 380%, whereas the activatable Gd-based agent experiences an r_1 change of <15%. At 1.4 T, the r_1 change is also much greater for the Mn−JED system (790%) than for Gd-bis-5HT-DTPA (60%). Images of phantoms prepared in human blood plasma exhibit comparable contrast (Figure S15).

To our knowledge, JED is the only chelator capable of stabilizing both Mn^{3+} and Mn^{2+} in the physiological milieu, and it enables rapid and reversible biochemically mediated interconversion between Mn^{3+} (low r_1) and Mn^{2+} (high r_1). The biochemically mediated r_1 change observed with Mn−JED is the largest of any activatable Gd- or Mn-based contrast agent. Peroxidase-mediated oxidation of Mn^{2+}-JED to Mn^{3+}-JED provides over an order of magnitude greater r_1 change than the state-of-the-art Gd-based peroxidase sensor and is achieved in minutes at peroxidase concentrations 1000-fold below what

DOI: 10.1021/jacs.6b10898
J. Am. Chem. Soc. 2016, 138, 15861−15864

is seen in vivo. Mn−JED offers a promising new paradigm for activatable MRI contrast agent development.

■ ASSOCIATED CONTENT

Supporting Information

The Supporting Information is available free of charge on the ACS Publications website at DOI: 10.1021/jacs.6b10898.

Experimental details, synthetic procedures, compound characterization, structures not depicted in the text, additional spectra, HPLC traces, and MRI acquisition parameters (PDF)

■ AUTHOR INFORMATION

Corresponding Author

*egale@nmr.mgh.harvard.edu

ORCID

Eric M. Gale: 0000-0003-4567-1126

Notes

The authors declare no competing financial interest.

■ ACKNOWLEDGMENTS

This work was supported by grants from the National Heart, Lung, and Blood Institute (K25HL128899) and the National Institute of Biomedical Imaging and Bioengineering (R01EB009062 and R21EB022804) and instrumentation funded by the National Center for Research Resources and the Office of the Director (P41RR014075, S10RR023385, and S10OD010650).

■ REFERENCES

(1) Boros, E.; Gale, E. M.; Caravan, P. *Dalton Trans.* **2015**, *44*, 4804.
(2) Angelovski, G. *Angew. Chem., Int. Ed.* **2016**, *55*, 7038.
(3) Caravan, P. *Acc. Chem. Res.* **2009**, *42*, 851.
(4) De Leon-Rodriguez, L. M.; Lubag, A. J. M.; Malloy, C. R.; Martinez, G. V.; Gillies, R. J.; Sherry, A. D. *Acc. Chem. Res.* **2009**, *42*, 948.
(5) Tsitovich, P. B.; Burns, P. J.; McKay, A. M.; Morrow, J. R. *J. Inorg. Biochem.* **2014**, *133*, 143.
(6) Do, Q. N.; Ratnakar, S. J.; Kovács, Z.; Sherry, A. D. *ChemMedChem* **2014**, *9*, 1116.
(7) Lubag, A. J. M.; De León-Rodríguez, L. M.; Burgess, S. C.; Sherry, A. D. *Proc. Natl. Acad. Sci. U. S. A.* **2011**, *108*, 18400.
(8) Lee, T.-Y.; Cai, L. X.; Lelyveld, V. S.; Hai, A.; Jasanoff, A. *Science* **2014**, *344*, 533.
(9) Huang, S.; Chen, H. H.; Yuan, H.; Dai, G.; Schühle, D. T.; Mekkaoui, C.; Ngoy, S.; Liao, R.; Caravan, P.; Josephson, L.; Sosnovik, D. E. *Circ. Cardiovasc. Imaging* **2011**, *4*, 729.
(10) Hingorani, D. V.; Bernstein, A. S.; Pagel, M. D. *Contrast Media Mol. Imaging* **2015**, *10*, 245.
(11) Yu, J.; Martins, A. F.; Preihs, C.; Clavijo Jordan, V.; Chirayil, S.; Zhao, P.; Wu, Y.; Nasr, K.; Kiefer, G. E.; Sherry, A. D. *J. Am. Chem. Soc.* **2015**, *137*, 14173.
(12) Nivorozhkin, A. L.; Kolodziej, A. F.; Caravan, P.; Greenfield, M. T.; Lauffer, R. B.; McMurry, T. J. *Angew. Chem., Int. Ed.* **2001**, *40*, 2903.
(13) Ekanger, L. A.; Ali, M. M.; Allen, M. J. *Chem. Commun.* **2014**, *50*, 14835.
(14) Ekanger, L. A.; Polin, L. A.; Shen, Y.; Haacke, E. M.; Martin, P. D.; Allen, M. J. *Angew. Chem., Int. Ed.* **2015**, *54*, 14398.
(15) Tsitovich, P. B.; Spernyak, J. A.; Morrow, J. R. *Angew. Chem., Int. Ed.* **2013**, *52*, 13997.
(16) Loving, G. S.; Mukherjee, S.; Caravan, P. *J. Am. Chem. Soc.* **2013**, *135*, 4620.
(17) Gale, E. M.; Mukherjee, S.; Liu, C.; Loving, G. S.; Caravan, P. *Inorg. Chem.* **2014**, *53*, 10748.
(18) Aime, S.; Botta, M.; Gianolio, E.; Terreno, E. *Angew. Chem., Int. Ed.* **2000**, *39*, 747.
(19) Yu, M.; Ambrose, S. L.; Whaley, Z. L.; Fan, S.; Gorden, J. D.; Beyers, R. J.; Schwartz, D. D.; Goldsmith, C. R. *J. Am. Chem. Soc.* **2014**, *136*, 12836.
(20) Yu, M.; Beyers, R. J.; Gorden, J. D.; Cross, J. N.; Goldsmith, C. R. *Inorg. Chem.* **2012**, *51*, 9153.
(21) Jackson, T. A.; Karapetian, A.; Miller, A.-F.; Brunold, T. C. *J. Am. Chem. Soc.* **2004**, *126*, 12477.
(22) Lauffer, R. B. *Chem. Rev.* **1987**, *87*, 901.
(23) Lacoste, R. G.; Christoffers, G. V.; Martell, A. E. *J. Am. Chem. Soc.* **1965**, *87*, 2385.
(24) Hamm, R. E.; Suwyn, M. A. *Inorg. Chem.* **1967**, *6*, 139.
(25) Frost, A. E.; Freedman, H. H.; Westerback, S. J.; Martell, A. E. *J. Am. Chem. Soc.* **1958**, *80*, 530.
(26) Jones, D. P.; Carlson, J. L.; Mody, V. C., Jr.; Cai, J.; Lynn, M. J.; Sternberg, P., Jr. *Free Radical Biol. Med.* **2000**, *28*, 625.
(27) Kirlin, W. G.; Cai, J.; Thompson, S. A.; Diaz, D.; Kavanagh, T. J.; Jones, D. P. *Free Radical Biol. Med.* **1999**, *27*, 1208.
(28) Drahoš, B.; Lukeš, I.; Tóth, E. *Eur. J. Inorg. Chem.* **2012**, *2012*, 1975.
(29) Gale, E. M.; Atanasova, I.; Blasi, F.; Ay, I.; Caravan, P. *J. Am. Chem. Soc.* **2015**, *137*, 15548.
(30) Bihari, S.; Smith, P. A.; Parsons, S.; Sadler, P. J. *Inorg. Chim. Acta* **2002**, *331*, 310.
(31) Rorabacher, D. B. *Chem. Rev.* **2004**, *104*, 651.
(32) Caravan, P.; Farrar, C. T.; Frullano, L.; Uppal, R. *Contrast Media Mol. Imaging* **2009**, *4*, 89.
(33) Su, H. S.; Nahrendorf, M.; Panizzi, P.; Breckwoldt, M. O.; Rodriguez, E.; Iwamoto, Y.; Aikawa, E.; Weissleder, R.; Chen, J. W. *Radiology* **2012**, *262*, 181.
(34) Nahrendorf, M.; Sosnovik, D.; Chen, J. W.; Panizzi, P.; Figueiredo, J.-L.; Aikawa, E.; Libby, P.; Swirski, F. K.; Weissleder, R. *Circulation* **2008**, *117*, 1153.
(35) Breckwoldt, M. O.; Chen, J. W.; Stangenberg, L.; Aikawa, E.; Rodriguez, E.; Qiu, S.; Moskowitz, M. A.; Weissleder, R. *Proc. Natl. Acad. Sci. U. S. A.* **2008**, *105*, 18584.
(36) DeLeo, M. J., III; Gounis, M. J.; Hong, B.; Ford, J. C.; Wakhloo, A. K.; Bogdanov, A. A., Jr. *Radiology* **2009**, *252*, 696.
(37) Daugherty, A.; Dunn, J. L.; Rateri, D. L.; Heinecke, J. W. *J. Clin. Invest.* **1994**, *94*, 437.
(38) Bourgeois, M.; Rajerison, H.; Guerard, F.; Mougin-Degraef, M.; Barbet, J.; Michel, N.; Cherel, M.; Faivre-Chauvet, A.; Gestin, J.-F. *Nucl. Med. Rev.* **2011**, *14*, 90.
(39) Kuppusamy, P.; Li, H.; Ilangovan, G.; Cardounel, A. J.; Zweier, J. L.; Yamada, K.; Krishna, M. C.; Mitchell, J. B. *Cancer Res.* **2002**, *62*, 307.
(40) Jorgenson, T. C.; Zhong, W.; Oberley, T. D. *Cancer Res.* **2013**, *73*, 6118.
(41) Rodríguez, E.; Nilges, M.; Weissleder, R.; Chen, J. W. *J. Am. Chem. Soc.* **2010**, *132*, 168.

DOI: 10.1021/jacs.6b10898
J. Am. Chem. Soc. 2016, 138, 15861−15864